A SIRIO-2 LASER RANGING EXPERIMENT

J. M. Dow W. Flury

European Space Operations Centre (ESOC)
Darmstadt, Federal Republic of Germany

ABSTRACT

On the basis of existing orbit determination software, ESOC is preparing to make use of laser ranging data from the SIRIO-2 LASSO experiment (Laser Synchronisation from Stationary Orbit). Four areas have been proposed for investigation: precise orbit determination, improvement of resonant gravity coefficients, polar motion, and calibration of the ESA VHF ranging system. The paper outlines the aims of this off-line software experiment and the preparations under way in support of them.

Keywords: Laser ranging, orbit determination, Earth gravity field, polar motion, ionospheric models, VHF ranging, calibration.

1. INTRODUCTION

The clock synchronisations to be carried out with the SIRIO-2 spacecraft by means of laser ranging (LASSO = Laser Synchronisation from Stationary Orbit) offer a unique opportunity for high precision determination of a geostationary orbit, using tracking data of decimeter or sub-decimeter accuracy. Starting from the basis of existing operational software, a proposal was made by ESOC to use this laser ranging data for four related experiments, whose objectives would be:

1) Precise orbit determination:
   - to determine accurately the orbit from laser ranging measurements;
   - to assess the achievable orbit accuracy;
   - to compare with radio tracking.
2) Determination of gravity coefficients:
   - to try to obtain improved estimates of resonant gravity coefficients;
   - to assess the effect of improved gravity coefficients on orbit accuracy.
3) Polar motion:
   - to determine polar motion using laser ranging measurements;
   - to evaluate the effect of improved modelling of polar motion on orbit determination accuracy;
4) Ionospheric calibration:
   - to calibrate the ESA VHF tracking system;
   - to evaluate the performance of the calibrated radio system.

In principle, none of these experiments will interfere with the normal mission operations of the spacecraft, since the laser and VHF ranging data are collected in support of the basic mission. However, since the time synchronizations will normally be carried out during one hour/day, additional ranging data will be required in order to give round-the-orbit coverage during at least some orbits.

The paper explains the experiment aims and describes the preparations under way in support of them.

2. PRECISE ORBIT DETERMINATION

2.1 Introduction

In the past, ESOC has performed orbit determination for several geostationary satellites (GEOS 2, OTS, METEOSAT, GOES) with radio tracking in VHF and/or S-band (accuracy from some metres to hundreds of metres in range). Laser ranging to a geostationary spacecraft sets new standards of accuracy on software models and processing methods.

2.2 Perturbations on the geostationary orbit

The principle perturbing forces acting on the geostationary orbit arise from:

- anomalies in the earth's gravity field;
- the gravitational fields of the Sun and the Moon;
- solar radiation pressure.

The earth gravity field is considered in detail in Section 3. It generates mainly in-plane perturbations.

Sun and Moon cause short period variations of the semi-major axis with amplitudes near 500m and 1200m respectively. More important are the per-

Proc. Int. Symp. Spacecraft Flight Dynamics, Darmstadt, FRG, 18-22 May 1981 (ESA SP-160, Aug. 1981)

turbations of the node and inclination. There is a forced precession of the orbit normal with a period of about 52 years. In a first approximation, the orbit pole performs a circular motion centred at right ascension 270° and declination 82.5°. The inclination of an initially equatorial geostationary orbit will reach a maximum near 15°.

Solar radiation pressure mainly affects the semi-major axis (short period) and eccentricity vector (annual effect). The magnitudes depend linearly on the spacecraft area-to-mass ratio. For an effective cross-section of 1.5m² and mass of 230 kg (SIRIO-2), the perturbations have amplitudes

$$\delta a \sim 23\text{m}$$
and $$a\delta e \sim 5500\text{m}$$

An initially circular orbit develops an eccentricity with the line of apsides maintained orthogonal to the sun direction. The eccentricity reaches its maximum amplitude after 6 months, and returns to zero after 1 year, see Ref. 1.

The tangential accelerations at 25°W and 20°E (the two positions foreseen for SIRIO-2) are 0.25×10^{-10} and -0.53×10^{-10}km/s² respectively. By comparison the total acceleration due to solar radiation pressure is about 0.5×10^{-10}km/s². The acceleration due to the Earth albedo radiation pressure is about two orders of magnitude less than this.

2.3 Radiation pressure model

A critical factor in our proposed experiment is thus the feasibility of accurately modelling the radiation pressure perturbation. The main problems are:

i) Data defining the physical properties (absorption, reflection, emission) of the spacecraft surfaces are not usually available except for normal incidence. The distribution of reflected radiation as a function of angle from the normal to the surface is not known (amount of specular versus diffuse reflection).

ii) Ageing of the materials after launch causes the values of these data to change.

iii) Most spacecraft have non-convex surfaces due to antennae and other appendages, so that shadowing and multiple reflections can be significant, and models become rather complex.

On the other hand, due to the nature of the perturbation on the orbit, it is hardly feasible to identify more than one or two parameters of such a model from the tracking data.

A model for SIRIO-2 has been developed assuming a somewhat idealized configuration consisting of (see fig. 1)
- the main body, a cylinder;
- the flat antenna, inclined at angle of 45° with respect to the spin axis, and supported by a rod of negligible surface area;
- the launcher adapter and ABM nozzle, considered as truncated cones. The nozzle furthermore is divided into two parts with different optical properties (see Table 1).

The forces are calculated according to the formula

$$\hat{f} = -k(R) \iint \left[\cos\theta\right] \{(a+2c\cos\theta)\hat{n}+b\hat{s}\}\, dA$$

where k(R) is the solar constant at distance R

$$= \frac{k_o}{R_e^2}, \quad k_o = \text{solar constant at 1 AU}, \quad R_e = \text{earth-sun distance in AU}$$

$\hat{n}$ = unit vector perpendicular to the surface element dA

$\hat{s}$ = unit vector pointing to Sun

$\cos\theta = \hat{n}.\hat{s}$

$$a = \frac{2}{3}\left[\gamma(1-\beta) + k(1-\gamma)\right]$$

$b = 1 - \beta\gamma$

$c = \beta\gamma$

γ = fraction of photons which are reflected

$\beta\gamma$ = fraction of photons which are specularly reflected (diffuse reflection is according to Lambert's cosine law)

$$k = \frac{e_f T_f^4 - e_b T_b^4}{e_f T_f^4 + e_b T_b^4}$$

e_f, e_b = emissivities of front and back surfaces

T_f, T_b = temperatures of front and back surfaces

Due to the lack of data, k has been taken = 0.

Shadow effects are taken into account, both as regards eclipses by the earth and shadows cast by parts of the spacecraft on other parts, with the following restrictions:
- no penumbra effects are considered, neither are the associated thermal effects;
- the forces on those parts of the spacecraft which are at times partly covered by shadows are calculated under the assumption that the ratio of the forces on the illuminated area and the forces on the whole area = the ratio of the corresponding projected areas.

Multiple reflections are not considered but should not be important.

The forces acting on those parts of the spacecraft which are solids of revolution only depend on the declination of the sun, whereas the force acting in the antenna also depends on the position of the spacecraft in its orbit.

Figs. 2 and 3 show the total acceleration and perturbation in position over 10 days around the summer solstice. The components of the latter are shown separately (radial Δr, tangential Δt, normal Δn). The extreme cases of totally diffuse or totally specular reflection are shown, using the data of Table 1. The difference between the two sets of curves is $\sim 20\%$ in position over this time interval.

Further details are given by Anselmi (Ref. 2). In order to save computation time during orbit determination, tables of the radiation pressure acceleration as a function of time of year and position in the orbit will be generated in advance, using an appropriate set of values for the surface properties. A multiplicative free parameter will be estimated during each orbit determination to further reduce the influence of modelling errors.

Table 1 - SIRIO-2 surface properties

Element	Absorption coeff.	Emissivity ε	Total surface area(m^2)
ABM nozzle (upper)	0.938	0.826	0.211
ABM nozzle (lower)	0.109	0.165	0.092
Launcher adapter	0.314	0.264	0.871
Solar array(i)upper	0.817	0.801	2.204
(cylinder)(ii)lower	0.814	0.812	2.105
Upper base	0.315	0.44	1.409
Lower base	0.315	0.44	1.27
Flat antenna	0.2	0.88	0.554

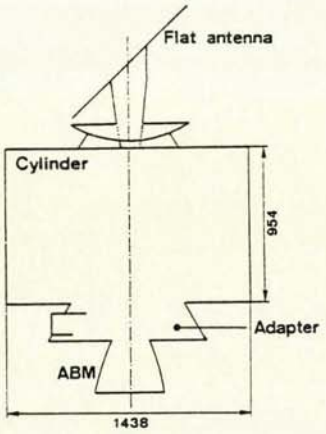

Fig.1 Schematic view of Sirio-2 spacecraft

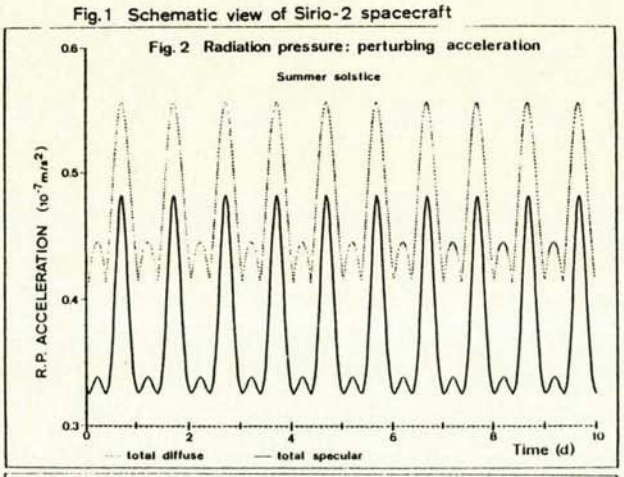

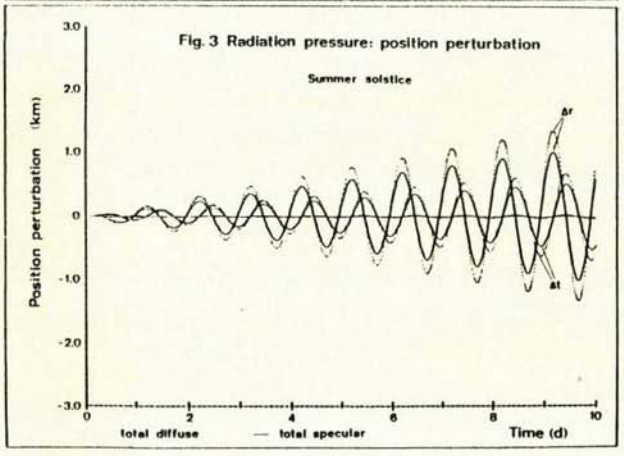

2.4 Coordinate system

The usual reference frame for satellite orbit calculations adopts the equatorial plane as fundamental plane and the equations of motion are integrated as if the reference frame were inertial. For precise orbit computations, the rotations represented by precession and nutation must be carefully taken into account.

A convenient reference frame is defined by the instantaneous equator and equinox of date Σ_t, since (apart from polar motion, which does not come into the orbit integration) this is the frame in which the satellite observations are made. In this non-inertial frame the equations of motion of the spacecraft with position vector $\hat{r}$ are

$$\ddot{\hat{r}} = \hat{F} - 2\hat{\omega} \times \dot{\hat{r}} - \dot{\hat{\omega}} \times \hat{r} - \hat{\omega} \times (\hat{\omega} \times \hat{r})$$

where $\hat{F}$ = perturbing accelerations and $\hat{\omega}$ = angular velocity of Σ_t relative to the mean system $\bar{\Sigma}_{t_o}$ at some epoch t_o.

The angular rotation vector relative to the mean system of date is

$$\hat{\omega}(\Sigma_t/\bar{\Sigma}_t) = (\dot{\bar{\varepsilon}}\cos\delta\psi - \dot{\varepsilon})\hat{1}_1 + (\dot{\bar{\varepsilon}}\cos\varepsilon\sin\delta\psi + \delta\dot{\psi}\sin\varepsilon)\hat{1}_2 + (\dot{\bar{\varepsilon}}\sin\varepsilon\sin\delta\psi - \delta\dot{\psi}\cos\varepsilon)\hat{1}_3$$

where ε=true obliquity, $\bar{\varepsilon}$=mean obliquity and $\delta\psi$=nutation in longitude. $\delta\varepsilon = \varepsilon - \bar{\varepsilon}$ is known as the nutation in obliquity. The unit vector $\hat{1}_1$ points to the instantaneous vernal equinox and $\hat{1}_3$ is the unit vector along the instantaneous Earth rotation axis. E.W. Woolard (ref. 3) has computed the expressions for $\delta\psi$ and $\delta\varepsilon$. They comprise 109 sine and cosine terms (69 for $\delta\psi$, 40 for $\delta\varepsilon$). The principal term in longitude has an amplitude of 17".2 and in obliquity of 9".2 with a period of 18.6 years.

The angular velocity relative to the mean system at epoch can be written as

$$\hat{\omega}(\Sigma_t/\bar{\Sigma}_{t_o}) = \hat{\omega}(\Sigma_t/\bar{\Sigma}_t) + N\hat{\omega}(\bar{\Sigma}_t/\bar{\Sigma}_{t_o})$$

N denotes the nutation matrix and connects true and mean equatorial frame of date:

$$N = R_1(-\varepsilon)R_3(-\delta\psi)R_1(\bar{\varepsilon})$$

$\hat{\omega}(\bar{\Sigma}_t/\bar{\Sigma}_{t_o})$ takes into account precession between t_o and t. For details see ref. 4.

Since $\hat{\omega}$ and $\dot{\hat{\omega}}$ enter the differential equations, also the second time derivatives of the transformation angles are required. For practical applications the epoch t_o is selected and $\hat{\omega}$ and $\dot{\hat{\omega}}$ are computed once and for all for a sufficiently long period of time.

2.5 Stations coordinates and tidal deflections

It is obvious that for orbit determination of a geostationary satellite by ranging from ground points, accurate coordinates for the ground points have to be known in advance. Due to the fixed geometry of the satellite-ground station configuration only the component of station position errors lying in the direction station-satellite could give a signature to the tracking

residuals, and this would be indistinguishable from a fixed bias. Consequently there is no possibility of estimating the station coordinates from the tracking data.

The positions of most existing laser stations have been determined by means of several coordinated campaigns (EDOC, EROS,...) whose aim was to locate the stations in a uniform geodetic datum. Both Transit doppler and satellite laser ranging techniques (LAGEOS, STARLETTE, GEOS 3) have been extensively used for this purpose.

The solid Earth is not perfectly rigid. The lunar and solar tides cause displacements on the Earth's surface of a few decimetres. Since laser ranging may reach accuracies of a few centimeters the tidal deflection of the station coordinates has to be modelled.

The differential gravity potential of Sun and Moon at a station (R, β, λ) may be written as (R = radius, β = geocentric latitude, λ = geographic longitude):

$$\phi_T = \frac{\mu_{\mathbb{C}}}{r_{\mathbb{C}}^3} R^2 \left[P_2(\cos\psi_{\mathbb{C}}) + \frac{R}{r_{\mathbb{C}}} P_3(\cos\psi_{\mathbb{C}})\right] + \frac{\mu_\odot}{r_\odot^3} R^2 \left[P_2(\cos\psi_\odot) + \frac{R}{r_\odot} P_3(\cos\psi_\odot)\right].$$

Terms of order $\frac{R^4}{r_{\mathbb{C}}^5}$ and $\frac{R^4}{r_\odot^5}$ are ignored. $\psi_\odot$ and $\psi_{\mathbb{C}}$ are the geocentric angles station - Sun and station-Moon, respectively. $r_\odot$ and $r_{\mathbb{C}}$ are the geocentric distances of Sun and Moon. The station coordinate deflections are proportional to the tide-rising potential ϕ_T scaled by the local gravity. Takeuchi (Ref. 5) gives the following expressions:

$$\Delta R = \frac{h}{g}\,\phi_T$$

$$\Delta\beta = \frac{l}{gR}\,\frac{\partial\phi_T}{\partial\beta}$$

$$\Delta\lambda = \frac{l}{gR\cos\beta}\,\frac{\partial\phi_T}{\partial\lambda}$$

h and l are known as Love and Shida numbers:

$$h = 0.60 \pm 0.1$$

$$l = 0.075 \pm 0.005.$$

The gravity acceleration may be calculated from

$$g\ [\mathrm{cm/sec^2}] = 978.0264\ (1 + 0.00530244\ \sin^2\beta + 0.00001196\ \sin^2 2\beta\ ).$$

For stations located substantially above the geoid, the gravity acceleration should be corrected for Bouguer anomalies.

Differentiation of ϕ_T leads to (Ref. 6):

$$\Delta R = \frac{h}{g}\,\phi_T$$

$$\Delta\beta = \frac{l}{gR}\,(G_{\mathbb{C}}\ G'_{\mathbb{C}} + G_\odot\ G'_\odot)$$

$$\Delta\lambda = \frac{l}{gR\cos\beta}\,(G_{\mathbb{C}}\ G''_{\mathbb{C}} + G_\odot\ G''_\odot)$$

where

$$G_b = \frac{\mu_b}{r_b^3} R^2 \left[3\cos\psi_b - \frac{R}{r_b}\left(\frac{3}{2} - \frac{15}{2}\cos^2\psi_b\right)\right]$$

$$G'_b = \sin\delta_b\cos\beta - \cos\delta_b\sin\beta\cos(\theta - \alpha_b)$$

$$G''_b = -\cos\delta_b\cos\beta\sin(\theta - \alpha_b)$$

$$\cos\psi_b = \sin\delta_b\sin\beta + \cos\delta_b\cos\beta\cos(\theta - \alpha_b).$$

b stands for $\mathbb{C}$ and $\odot$. α_b and δ_b denote right ascension and declination. θ is the station's right ascension.

2.6 Outline of Software

The basic tool is the orbit determination program BAHN developed at ESOC as part of the Multi-satellite Support System (MSSS). This program uses the method of weighted least squares to apply differential corrections to an a priori estimate of the orbit. The state of the satellite at the epoch can be estimated in terms of cartesian coordinates or osculating Keplerian or equinoctial elements, and in addition, a wide variety of parameters can be improved. These include tracking measurement biases, parameters of ionospheric correction models, timing biases, station coordinates, pole position, parameters defining air drag and radiation pressure, selected components of an impulsive velocity increment, a correction factor to the nominal thrust applied during a long orbit manoeuvre, and selected components of an unknown perturbing acceleration assumed constant in spacecraft or inertial axes. Each parameter from a set of 129 is given the status 0, 1, or 2 indicating respectively: known with zero uncertainty; to be improved from a given initial value with specified uncertainty; to be considered to have a fixed value but of non-zero uncertainty. Thus parameters of the last class permit the computation of a realistic covariance matrix for the estimate parameters without overburdening the estimation process with observability and other numerical problems.

For the SIRIO-2 experiment the orbit will be integrated in the true-of-date system by an eighth-order multi-step method (Adams-Bashforth) Adams-Moulton) with the Runge-Kutta-Fehlberg 7(8) method as starting procedure. According to the options chosen the following perturbations can be included: earth potential up to given degree n and order m; luni-solar gravity; air drag; radiation pressure; manoeuvres (impulsive or otherwise) due to the attitude and orbit control system; and a constant acceleration given in spacecraft or inertial axes.

A number of different types of tracking data can be handled by the program (combinations of 1-, 2-, and 4-way range; range-rate or range-difference; azimuth and elevation; GRARR antenna angles; and interferometer measurements). In addition to the corrections made at the pre-processing stage, i.e. those independent of orbital position or station position, corrections for polar motion, ionospheric and tropospheric refraction, propagation time delay, and ambiguity resolution errors can be performed, and the measurements edited according to various criteria.

2.7 Conduct of the Experiment

Orbit determination using the laser data will be carried out on a regular basis. The optimal arc length for a determination will depend on the accuracy of the models and of the software in general. The frequency with which the orbit determination will be done will also depend on the availability of the laser data (utilisation of LASSO, weather conditions,...).

From orbit determinations over adjacent and overlapping arcs, and the information contained in the state covariance matrix, the accuracy of the determined orbit will be estimated.

3. DETERMINATION OF GEOPOTENTIAL COEFFICIENTS

3.1 Introduction

A convenient formulation of the Earth gravitational potential is the series expansion in spherical harmonics (Ref. 7)

$$V = \frac{GM}{r} + \sum_{\ell=2}^{\infty} \sum_{m=o}^{\ell} \sum_{p=o}^{\ell} \sum_{q=-\infty}^{+\infty} V_{\ell mpq} = \frac{GM}{r} + R ,$$

where

$$V_{\ell mpq} = \frac{GM}{a}\left(\frac{Re}{a}\right)^{\ell} F_{\ell mp}(i)\, G_{\ell pq}(e) S_{\ell mpq}(\omega, M, \Omega, \theta)$$

$$S_{\ell mpq} = \begin{bmatrix} C_{\ell m} \\ -S_{\ell m} \end{bmatrix} \begin{matrix} (\ell-m)\text{even} \\ (\ell-m)\text{odd} \end{matrix} \cos\psi + \begin{bmatrix} S_{\ell m} \\ C_{\ell m} \end{bmatrix} \begin{matrix} (\ell-m)\text{even} \\ (\ell-m)\text{odd} \end{matrix} \sin\psi$$

$$\psi = (\ell - 2p)\omega + (\ell - 2p+q)\, M + m\,(\Omega - \theta).$$

In these equations a, e, i, Ω, ω, M are the osculating Kepler elements, GM the product of Earth mass and gravitational constant, R_e the mean equatorial radius, θ the Greenwich sidereal time, $F_{\ell mp}(i)$ the inclination function and $G_{\ell pq}(e)$ the eccentricity function. $G_{\ell pq}(e)$ is of the order of $e^{|q|}$, thus only a few terms are required in eccentricity expansions for near-circular orbits.

The index ℓ designates the degree while m the order of a spherical harmonic

$$V_{\ell m} = \sum_{p=o}^{\ell} \sum_{q=-\infty}^{+\infty} V_{\ell mpq}$$

$C_{\ell m}$ and $S_{\ell m}$ are constants to be determined from observation of satellite orbits. $J_2 = -C_{20}$ takes the largest value of 1.082×10^{-3} while the other coefficients are of the order of 10^{-6}.

The determination of the gravity coefficients is a two stage process: the zonal coefficients (m=0) are first estimated, followed by tesseral and sectorial coefficients. Current earth gravity models give spherical harmonic expansions up to (36,36) (GEM 10B, SEASAT models PGS 1 to 4). GEM 10 (592 coefficients) is complete to degree and order 22 with some selected higher degree coefficients.

The calculation of a gravity solution is a formidable task. First several hundred thousands of observations are processed. Subsequently a system of equations with several hundreds of unknowns is established. The unknowns comprise not only the gravity coefficients but also coordinates of stations providing tracking data. The accuracy of the individual coefficients derived is therefore questionable, particularly those of higher degree and order.

An independent check of the validity of a solution can be made with resonant orbits, i.e. orbits with an exactly or nearly repeating ground-track.

Mathematically, resonance can be described by the condition $s(\dot{\theta} - \dot{\Omega}) = \dot{M} + \dot{\omega}$. Thus s is essentially the number of satellite revolutions during one day. If s is an integer then the orbit repeats exactly after s nodal revolutions.

For q = o the time derivative of the argument of the disturbing function becomes

$$\dot{\psi} = (\ell-2p)(\dot{\omega}+\dot{M}) + m(\dot{\Omega}-\dot{\theta}),$$

which vanishes for $s = \frac{m}{\ell-2p}$.

In linear perturbation theories $\dot{\psi}$ appears as divisor in the element perturbations.

For exact commensurability $\dot{\psi}$ vanishes and the classical perturbation theory breaks down. Special provisions have to be made to cope with this case. For a near-resonance orbit ψ is small and consequently the element perturbation large.

Thus for resonance or near-resonance the perturbing effect of certain spherical harmonics is significantly increased. This property can be exploited in the reverse direction to estimate the spherical harmonic coefficients from the perturbations of a resonance orbit.

For geostationary orbits we have s = 1 or l-m = 2p. Thus resonance occurs with

$$(l,m) = \{(2,2), (3,1), (3,3), (4,2),..\}.$$

The effect of the harmonics is attenuated by the factor $\frac{Re}{a} = \frac{1}{6.61}$ between consecutive degrees.

The case of the geostationary orbit is fortunate in that the effect of the non-resonant spherical harmonics is extremely small due to the large distance Earth-satellite. Thus only a few spherical harmonics have a significant effect at the geostationary distance. With accurate tracking techniques the estimation of the gravity coefficients could be a rather simple task compared to near-earth satellites where a large number of spherical harmonics are involved.

After several tens of geostationary satellites in order there is still a considerable uncertainty in the knowledge of the resonance gravity coefficients. For station-keeping and long-term orbit prediction a precise model of the anomalous earth gravity field is desirable.

3.2 Resonance Perturbations of Geostationary Satellites

The dominant resonance perturbations of geostationary satellites affect the semi-major axis and the mean longitude. For 1:1 resonance of near-circular orbits the potential terms with indices q = 0, m = ℓ-2p give rise to an almost constant longitudinal acceleration.

The resonant disturbing function can be written as

$$R = \frac{GM}{\varepsilon} \sum_{\substack{\ell,m \\ (\ell-m)\text{even}}} J_{\ell m} \left(\frac{Re}{a}\right)^{\ell} F_{\ell m,\frac{\ell-m}{2}}(i)\, G_{\ell,\frac{\ell-m}{2},o}(e) \times \cos m\,(\lambda - \lambda_{\ell m} - \theta),$$

where

$$J_{\ell m} = \sqrt{C_{\ell m}^2 + S_{\ell m}^2}$$

$$\lambda_{\ell m} = \frac{1}{m} \tan^{-1}\left(\frac{S_{\ell m}}{C_{\ell m}}\right)$$

$$\lambda = \Omega + \omega + M = \text{mean longitude.}$$

The rate of change of the semi-major axis is

$$\dot{a} = \frac{2}{na} \frac{\partial R}{\partial \lambda} = -\frac{2}{na} \sum_{\substack{\ell,m \\ (\ell-m)\text{even}}} m\, Q_{\ell m} \sin m\,(\lambda - \lambda_{\ell m} - \theta)$$

where

$$Q_{\ell m} = \frac{GM}{a} J_{\ell m} \left(\frac{Re}{a}\right)^{\ell} F_{\ell m,\frac{\ell-m}{2}}(i)\; G_{\ell,\frac{\ell-m}{2},o}(e) .$$

Since the arguments of the trigonometric functions are slowly varying, the rate of change $\dot{a}$ is almost constant for some period of time.

For a description of the longitude history the second derivative is required:

$$(\lambda-\theta)^{\cdot\cdot} = \ddot{\lambda} \doteq \frac{\partial n}{\partial a}\dot{a} = \frac{3}{a^2} \sum_{\substack{\ell,m \\ (\ell-m)\text{even}}} m\, Q_{\ell m} \sin m\,(\lambda-\lambda_{\ell m}-\theta)$$

In case of a triaxial Earth all $Q_{\ell m}$ disappear except for Q_{22}. The equatorial cross-section becomes an ellipse. It is convenient to change the longitude of the origin to the minor axis of the equatorial ellipse: $\bar{\lambda} = \lambda - \theta - \lambda_{22} \pm \frac{\pi}{2}$, so that

$$\ddot{\bar{\lambda}} + \frac{1}{2} k^2 \sin 2\bar{\lambda} = 0,$$

where $k^2 = 36\, n^2 J_{22} \left(\frac{R_e}{a}\right)^2$. This is analogous to the mathematical pendulum differential equation $\ddot{x} + g/l \sin x = 0$. The types of motion are libration (around the nearest equilibrium position) or circulation. The libration period is $T = \frac{4}{k} K(\sin \bar{\lambda}_m)$, where K is the complete elliptical integral of the first kind and $\bar{\lambda}_m$ the amplitude of the libration.

The pendulum-type motion provides a close approximation of the actual longitude evolution. Other resonance terms, luni-solar accelerations and solar radiation pressure merely represent perturbations.

3.3 Current Estimates of Resonance Coefficients

Table 2 shows the estimates of the second, third and fourth degree resonance coefficients (normalised). Table 3 lists references and geodetic constants used in the different models:

	Reference	GM(km^3/s^2)	R_e(km)
GEM 7 }	Ref. 8	398600.8	6378.145
GEM 8 }		398600.8	6378.145
GEM 10	Ref. 9	398600.47	6378.140
GRIM 2	Ref.10	398601.3	6378.155
SAO II	Ref.11	398601.3	6378.155
SAO 1980	Ref.12	398600.5	6378.136

Table 3 References and Geodetic Parameters

Correction for differing values of GM and Re does not affect the coefficients up to the degree and precision shown in Table 4. There is fair agreement among the C_{22} and S_{22} estimates, apart from GRIM 2 which gives a slightly larger value for C_{22}. The spread in the third and fourth degree coefficients is significant. The Goddard earth models tend to similar values while GRIM 2 and SAO II deviate considerably.

3.4 Estimation Approach

We outline three approaches to attack the problem. The most interesting is the first one where the longitude acceleration function is established in a first step using tracking data over a relatively short time span.

3.4.1 Short-Arcs

A promising approach for the determination of C_{lm}, S_{lm} is to calculate first the acceleration in longitude $\ddot{\lambda}$ which is linearly related to the coefficients. $\ddot{\lambda}$ can be derived from $\ddot{\lambda} = \frac{\partial \dot{n}}{\partial a}\dot{a}$, where $\frac{\partial \dot{n}}{\partial a}\dot{a}$ is calculated from the orbit determination results. $\ddot{\lambda}$, which depends on the geographical longitude Λ of the subsatellite point, should be determined in the ideal case for all longitudes $25^\circ W \leq \Lambda \leq 20^\circ E$.

During its lifetime SIRIO-2 will be positioned within the longitude band $25^\circ W \leq \Lambda \leq 20^\circ E$, hence the acceleration profile can only be established within this interval.

The coefficients C_{lm}, S_{lm} are determined from the function $\ddot{\lambda}(\Lambda)$, $25^\circ W \leq \Lambda \leq 20^\circ E$, either through Fourier analysis or least squares estimation. The solution obtained in this way is only valid within the interval $25^\circ W \leq \Lambda \leq 20^\circ E$. Hence we cannot expect to obtain a global improvement of the gravity coefficients. However within the "European longitude band" where the ESA satellites are located, a better knowledge of the gravity field should result.

3.4.2 Long Arcs

We assume the satellite is slowly drifting ($|\dot{\Lambda}| < 1^\circ$/day). Tracking data is collected over a longer period of time (some ten of days).

The list of solve-for variables in orbit determination comprises usually the state variables at epoch and possibly a measurement bias or spacecraft parameter (solar radiation pressure coefficient). In the long arc approach this list is augmented by the gravity coefficients C_{lm} and S_{lm}.

	$\bar{C}_{22}\times10^6$	$\bar{S}_{22}\times10^6$	$\bar{C}_{31}\times10^6$	$\bar{S}_{31}\times10^6$	$\bar{C}_{33}\times10^6$	$\bar{S}_{33}\times10^6$	$\bar{C}_{42}\times10^6$	$\bar{S}_{42}\times10^6$	$\bar{C}_{44}\times10^6$	$\bar{S}_{44}\times10^6$
GEM 7	2.4303	-1.3946	2.0296	0.2032	0.7263	1.4108	0.3465	0.6623	-0.1966	0.3063
GEM 8	2.4345	-1.3953	2.0317	0.2496	0.7162	1.4169	0.3473	0.6657	-0.1954	0.3053
GEM10	2.4340	-1.3991	2.0285	0.2520	0.7003	1.4125	0.3526	0.6627	-0.1966	0.2989
GRIM 2	2.4878	-1.3644	1.9617	0.1848	0.7124	1.5569	0.2974	0.6653	-0.0996	0.3865
SAO II	2.4129	-1.3641	1.9698	0.2601	0.6863	1.4304	0.3302	0.7063	-0.0797	0.3393
SAO 1980	2.4231	-1.3855	2.0378	0.2748	0.6708	1.4964	0.3567	0.6635	-0.1544	0.3053

Table 2 : Resonance Gravity Coefficients (normalised)

3.4.3 Lumped Gravity Coefficients

In this approach the non-spherical part of the gravity potential is approximated by the second harmonic and the second degree tesseral harmonic. Two best-fitting parameters $C_{\ell_{22}}$ and $S_{\ell_{22}}$ are estimated (or $J_{\ell_{22}}$ and $\lambda_{\ell_{22}}$).

This method was applied by Merson (Ref. 13) to estimate $J_{\ell_{22}}$ and $\lambda_{\ell_{22}}$ from SKYNET data in the longitude band 40°E to 50°E. The formula derived by Allan (Ref. 14) was applied (unnormalized coefficients):

$$\ddot{\lambda} = 18n^2 J_{\ell_{22}} \left(\frac{Re}{a}\right)^2 c^4 \sin 2(\lambda - \lambda_{\ell_{22}}^*)$$

$$-12n\dot{\lambda} J_{\ell_{22}} \left(\frac{Re}{a}\right)^2 c^2 (4c^2-1) \sin 2(\lambda - \lambda_{\ell_{22}}^*),$$

where n = mean motion and $c = \cos\frac{i}{2}$.

The left-hand side $\ddot{\lambda}$ is the observed acceleration in longitude which is the result of all tesseral harmonics. An approximation with the second degree tesseral harmonic will therefore produce different $J_{\ell_{22}}$ and $\lambda_{\ell_{22}}$ depending on the geographical longitude.

3.5 Conditions of the Experiment

It is clear that only a fixed linear combination of the resonant gravity coefficients can be observed if the spacecraft is maintained at a given longitude. Hence the gravity experiment has to be concentrated on the drift phase between the longitudes 25°W and 20°E. A slow drift of 1-2°/day and sufficiently frequent orbit determinations should allow at least some of the resonant coefficients to be determined.

Disturbances due to attitude and orbit control during this phase should as far as possible be avoided.

4. DETERMINATION OF POLAR MOTION

4.1 Introduction

Polar motion is the motion of the earth's spin axis relative to the earth's surface. In 1765 Leonhard Euler predicted a 305 day period assuming a rigid earth. The existence of polar motion was for the first time demonstrated by F. Küstner in 1888. In 1892 S.C. Chandler showed that the polar motion is composed of two oscillatory components with 12 months and 14.2 months period. The 14-month component is a free oscillation arising from the spheroidal shape of the earth. The 12-month component is a forced oscillation caused by meteorological effects. The amplitudes of both oscillations comprise a random part. Thus polar motion cannot be reliably predicted (Ref. 15). On the other hand a precise knowledge of the pole position is required for certain applications. For example, polar motion affects the position of tracking stations in an inertial frame, thus influences the accuracy of orbit determination.

Fig. 4 (from BIH Annual Report 1978) shows the path of the pole from 1977.0 until 1979.0. The linear dimension amounts to approximately 15 meters or 0".5.

In 1899 the International Latitude Service (ILS) was established to monitor the path of the pole. ILS comprises five stations which are all near 39° 08' north.

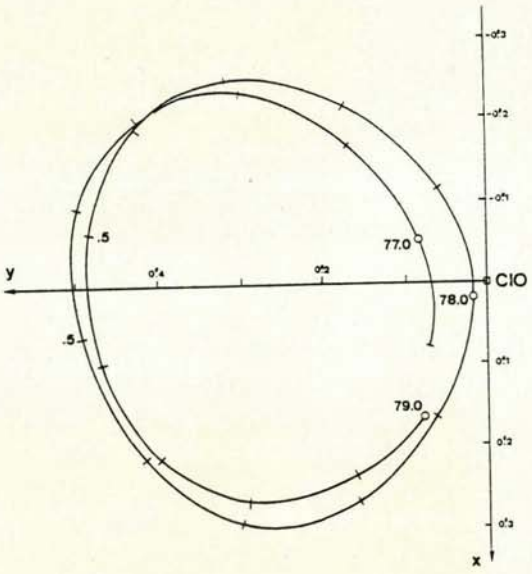

Fig. 4 Path of the pole from 1977.0 to 1979.0 (smoothed)

Beginning with 1962 IPMS (International Polar Motion Service) and BIH (Bureau International de l'Heure) provided more accurate determinations of the polar motion using astrometric methods.

Recent pole determinations use satellite observations, lunar laser ranging, or VLBI techniques. DMA (Defense Mapping Agency) derives pole coordinates from Doppler observation of NAVSAT spacecraft. At Goddard Space Flight Center and the University of Texas the pole position is determined from laser tracking of LAGEOS. These new methods are currently being compared systematically in the MERIT campaign (Ref. 16).

All space techniques are based on the fact that the equations of motion of the spacecraft are defined with respect to an inertial frame of reference. The ground-stations however are fixed to the earth and rotate around the actual spin axis. Ignoring the polar motion (pole coordinates m_1, m_2 on unit sphere) leads to apparent orbit perturbations (ref. 17)

$$\Delta i = m \sin(\Omega - \theta - \Psi)$$
$$\Delta(\omega + f) = m \cos(\Omega - \theta - \Psi)\operatorname{cosec} i$$
$$\Delta\Omega = m \cos(\Omega - \theta - \Psi)\operatorname{cotan} i$$

where $m = (m_1^2 + m_2^2)^{1/2}$, $\psi = \tan^{-1}(\frac{m_1}{m_2})$ and θ is the sidereal angle.

4.2 Observability of pole coordinates

The instantaneous position of the earth's spin axis is defined by the rotations x_p, y_p from the CIO along the Greenwich meridian (both assumed fixed with respect to the crust) and along the 90°W meridian, as shown in Fig. 5. The definition of the Earth-fixed reference system is inherent in the adopted values of the laser station coordinates.

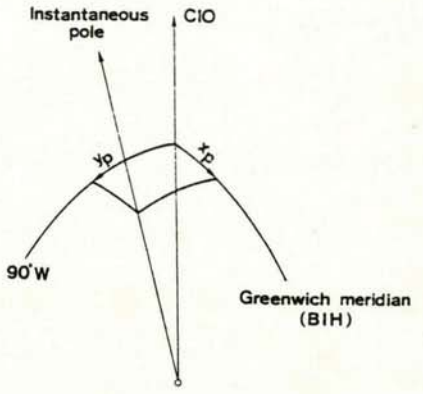

Fig. 5 Definition of pole coordinates x_p, y_p

Since x_p, y_p are small (typically <0".5, or 15m at the earth's surface), we can use the approximate transformation

$$\hat{x} = W\hat{x}_s$$

where $\hat{x}$ = station position in the true of date, equatorial system rotating with the earth (Σ_R system)

$\hat{x}_s$ = station position in CIO/Greenwich system

$$W = \begin{bmatrix} 1 & 0 & -x_p \\ 0 & 1 & y_p \\ x_p & -y_p & 1 \end{bmatrix}$$

If further $\hat{x}$ = spacecraft position in the Σ_R system, then the ranging measurements ρ are given by

$$\rho^2 = (\hat{x} - W\hat{x}_s)^2 = \hat{x}^2 - 2\hat{x}^T W\hat{x}_s + (W\hat{x}_s)^2$$

($\hat{x}^T$ denotes transpose of $\hat{x}$). Since $\hat{x}$ does not depend on x_p, y_p and $(W\hat{x}_s)^2$ is invariant under pure rotations, differentiation with respect to x_p, y_p gives

$$\rho d\rho = -\hat{x}^T dW\hat{x}_s$$
$$= -\hat{x}^T \begin{bmatrix} -Z_s dx_p \\ Z_s dy_p \\ X_s dx_p - Y_s dy_p \end{bmatrix}$$
$$= (xZ_s - zX_s)\, dx_p + (zY_s - yZ_s)\, dy_p \qquad (1)$$

i.e. $\frac{\partial \rho}{\partial x_p} = \frac{xZ_s - zX_s}{\rho}$, $\frac{\partial \rho}{\partial y_p} = \frac{zY_s - yZ_s}{\rho}$

For an equatorial orbit (z=o), (1) becomes

$$d\rho = \frac{Z_s}{\rho}(x dx_p - y dy_p)$$

which implies that for a geostationary satellite at a fixed longitude (constant x, y) always the same linear combination of the pole position errors δx_p and δy_p will appear in the measurement residuals $\delta\rho$, irrespective of the location and number of the tracking stations. Hence polar motion cannot be determined by ranging to a geostationary satellite. The individual components are well-observable, but the combination x_p, y_p is not, using a single spacecraft.

Assuming the orbital position and the y_p component to be precisely known, then the standard deviation of the ranging measurements maps onto the standard deviation of x_p by

$$\sigma_{x_p} = \left|\frac{\partial x_p}{\partial \rho}\right| \sigma_\rho$$
$$= \frac{\rho}{Z_s r_s |\cos\lambda|}\sigma_\rho$$
$$\sim \frac{2\sigma_\rho}{r_e |\cos\lambda|}$$

where r_s, r_e are the geostationary radius and earth radius respectively and λ = spacecraft longitude in the Σ_R system. The approximation is valid for a mid-latitude station.

Similarly if x_p is known

$$\sigma_{y_p} \sim \frac{2\sigma_\rho}{r_e |\sin\lambda|}$$

Hence for a geostationary satellite at λ=0 orπ, the y-component of the pole position could not be observed even if the x-component were assumed perfectly known. An analogous conclusion holds for $\lambda = \pm \pi/2$.

At the Sirio-2 longitudes 25°W and 20°E we find

$$\sigma_{x_p} \sim \frac{2\sigma_\rho}{r_e} \quad , \quad \sigma_{y_p} \sim \frac{4\sigma_\rho}{r_e}$$

Thus 10cm laser ranging accuracy would give 20cm and 40cm accuracy for the x- and y-components if they could be made separately observable.

4.3 Covariance Analysis

The partials for range measurements with respect to x_p, y_p and the facility for estimating or considering x_p, y_p have been implemented in the BAHN orbit determination program. Table 4 shows the results of some simulations using laser ranging data of 10cm. accuracy from the stations listed in Table 5. The observability of x_p, y_p is clearly shown by the a posteriori standard deviations $\sigma_{x_p}, \sigma_{y_p}$ derived from the estimate covariance in BAHN (a priori standard deviation assumed = 2").

Given that the currently achievable accuracy using Transit doppler tracking or Lageos laser ranging is better than 50cm or 0".017, it seems unlikely that for inclinations of 1° or less (SIRIO-2 value) a good determination of x_p, y_p is feasible, while with a 10° inclination, 2 stations would be enough to determine the pole position with high precision, provided the station positions can be determined independently with decimeter accuracy.

Table 5 Positions of laser stations used in Table 4.

Station	Name	East Longitude (deg)	Latitude (deg)
Kootwijk (NL)	KOO	5.81	52.18
GSFC (USA)	GSF	283.16	39.00
Grasse (F)	GRA	6.92	43.75
Calgiari (I)	CAL	8.97	39.13

5. CALIBRATION OF VHF SYSTEMS

5.1 ESA VHF Network

The ESA VHF tracking network comprises the 4 stations Redu, Kourou, Malindi, and Carnarvon (see Table 6). Its main function is the support of transfer and near-synchronous orbit phases of geostationary missions, but it may provide support in other cases where accuracy requirements are not very stringent, e.g. GEOS-1 12 hr. orbit, GEOS-2 SO, COS-B. All 4 stations have the same standardized hardware.

Table 6 Locations of ESA VHF Ranging Stations

Station	Country	East Longitude (deg)	Latitude (deg)
Redu	Belgium	5.14	50.00
Kourou	French-Guyana	-52.80	5.25
Malindi	Kenya	40.32	-2.99
Carnarvon	Australia	113.72	-24.90

Ranging support for SIRIO-2 in NSO and SO phases will be provided by Redu and Kourou. Malindi will also have good visibility of the spacecraft in both of its nominal positions (25°W and 20°E), but there are no plans to make routine use of this. There will be no visibility at Carnarvon.

5.2 Errors in VHF Ranging

The errors affecting VHF ranging measurements are

(1) delays due to atmospheric refraction (ionosphere, troposphere)

(2) delays due to the on-board transponder

(3) delays due to ground hardware (cables, filters,...)

(4) other random and systematic hardware effects (phase instabilities, phase measurement errors,...).

A special calibration loop at the station allows the errors (3) to be measured conveniently on a regular basis (ideally, before and after each ranging operation). The transponder delay (typically of the order of tens of μs, 1 μs corresponds to 300m) is calibrated on the ground before launch, and curves showing its variation as a function of relevant parameters (temperature, frequency, AGC) are normally available for use in range data preprocessing. Any other drift in the transponder delay after launch will however not be directly measurable.

Refraction in the troposphere causes a delay of approximately 2.5/sinE(m), where E = spacecraft elevation; the exact delay depends on local and regional atmospheric conditions (temperature, pressure, relative humidity). However since the total effect is small compared with the ionospheric effect at VHF, a simple a priori model for each station is in practice sufficient.

5.3 Ionosphere

The ionosphere is the highly ionized region of the atmosphere between altitudes 80 and 1000 km approximately. It can be shown that the ionospheric effect on a ranging measurement is a delay proportional to the total electron content along the signal path. Various theoretical and empirical models have been developed to model the electron density (e.g. Chapman, von Roos, Willman, Bent et al), which is in general a function of

(i) phase in the 11-year solar cycle (usually accounted for by 10.7 cm solar flux mean values) and sun spot activity (10.7 cm daily values)

(ii) latitude

(iii) local time

(iv) date.

The GSFC-Bent model used in the operational ESOC software approximates the electron density as a function of height by a curve consisting of five pieces (a bulge at the height of maximum density consisting of a bi-parabola on the bottom-side and a parabola on the top-side; a top-side decay modelled by three exponential functions).

Table 4 Covariance Analysis of Polar Motion Determination

Inclination (Deg)	Stations	Estimate Parameters	Consider Parameters	σ''_{x_p}	σ''_{x_p}
0.1	KOO,GSF,CAL	$\hat{x},\dot{\hat{x}},x_p,y_p$	-	0.430	0.920
0.1	KOO,GSF,CAL	y_p	-	-	0.002
0.1	KOO,GSF,CAL	x_p,y_p	-	0.263	0.563
0.1	KOO,GSF,CAL,GRA	x_p,y_p	-	0.244	0.525
1.0	KOO,GSF	$\hat{x},\dot{\hat{x}},x_p,y_p$	-	0.562	1.209
1.0	*KOO,GSF	$\hat{x},\dot{\hat{x}},x_p,y_p$	-	0.243	0.523
1.0	*KOO,GSF	$\hat{x},\dot{\hat{x}},c_R,x_p,y_p$	$\hat{x}_s(\sigma=0.5m)$	0.247	0.530
1.0	KOO,GSF,CAL,GRA	$\hat{x},\dot{\hat{x}},c_R,x_p,y_p$	-	0.055	0.115
1.0	KOO,GSF,CAL,GRA	$\hat{x},\dot{\hat{x}},x_p,y_p$	-	0.054	0.114
1.0	KOO,GSF,CAL,GRA	$\hat{x},\dot{\hat{x}},c_R,x_p,y_p$	$\hat{x}_s(\sigma=0.5m)$	0.292	0.535
1.0	*KOO,GSF,CAL,GRA	$\hat{x},\dot{\hat{x}},c_R,x_p,y_p$	$\hat{x}_s(\sigma=0.5m)$	0.072	0.141
1.0	ǂKOO,GSF,CAL,GRA	$\hat{x},\dot{\hat{x}},c_R,x_p,y_p$	$\hat{x}_s(\sigma=0.5m)$	0.047	0.095
10.0	KOO,GSF	$\hat{x},\dot{\hat{x}},c_R,x_p,y_p$	-	0.010	0.018
10.0	KOO,GSF	$\hat{x},\dot{\hat{x}},c_R,x_p,y_p$	$\hat{x}_s(\sigma=1m)$	0.037	0.053
10.0	KOO,GSF,GRA	$\hat{x},\dot{\hat{x}},c_R,x_p,y_p$	-	0.007	0.011

$\hat{x},\dot{\hat{x}}$ = position and velocity of spacecraft at epoch
c_R = radiation pressure coefficient
$\sigma_{x_p},\sigma_{y_p}$ = a posteriori standard deviations of estimates of x_p,y_p (arc sec)
Ranging accuracy of 10cm over 1 day 1/hr (perfect atmospheric conditions!)

* means ranging over 2 days, ǂ means ranging over 3 days

In periods of high solar activity (e.g. 1978-81) the ranging delay due to the ionosphere may be of the order of 500m for a spacecraft in the local zenith, so that for lower elevations corrections of up to 4 or 5 km may be necessary.

5.4 Calibration with SIRIO-2

Since the orbit of SIRIO-2 will be known with very high accuracy from the laser ranging measurements, and in particular the distance of the spacecraft from those regions where the lasers are situated, a very accurate reference is available to compare with the measured VHF ranges. It should also be noted that the locations of the reference points of the VHF ranging antennae at Redu, Kourou, and Malindi are known with a few meters accuracy from Transit doppler campaigns at the stations.

In making the comparison of computed and measured ranges, information could be gained on:

(1) the total delay in the VHF ranges due to hardware and ionosphere as a function of time of day (typical behaviour: rise to maximum around 14 hr local time, large fluctuations around sunrise and sunset, uniform low level during night)

(2) the accuracy of the corrections computed by the Bent and other models (shape of the function w.r.t. time of day, and magnitude at specific times).

(3) the stability of the ranging system.

Since the most important hardware delays should be removed by calibration, we are effectively studying the behaviour of the ionosphere in the region above the VHF ranging stations. It may be possible to develop simple empirical models for the ranging corrections required for SIRIO-2 at a single longitude.

5.5 Data Required

In principle there are no special requirements for data beyond the VHF ranging which will be carried out routinely in any case in support of SO operations. However it would greatly enhance the study of the VHF system if special VHF ranging campaigns could be carried out during which more intensive tracking is performed (e.g. every hour from each participating station during several consecutive days). The campaigns would be repeated at convenient intervals as necessary (e.g. monthly or less frequently). The optimal campaign durations and frequency will depend to some extent on the consistency of the measured delays themselves.

6. CONCLUSIONS

The SIRIO-2 laser ranging data will offer a fascinating challenge for precise orbit determination. By providing a rigorous test of our models it should lead to improved operational software.

It may be possible to determine the values of some resonant gravity coefficients if the solar radiation pressure can be modelled accurately enough and if sufficiently dense tracking is performed during a slow drift phase from the two spacecraft positions at 25°W and 20°E. Ideally no thrusters should be activated during the drift phase.

The aim of using SIRIO-2 for polar motion determination is probably not feasible with an accuracy comparable with that of the best methods currently available, at least during the initial low inclination phase. However with higher inclinations (e.g. 10°) the geosynchronous orbit could provide very precise polar motion determinations.

Finally SIRIO-2 provides an ideal opportunity to calibrate a general tracking facility (the VHF ranging network) which will be used to support all planned geostationary missions of ESA.

Acknowledgement

The support of Dr. A. Anselmi (Visiting Scientist at ESOC), who developed and implemented the radiation pressure model, is gratefully acknowledged.

This experiment is being performed within the framework of LEUT (LASSO Experimenters and Users Team), which is the group of principal investigators for the LASSO experiment. Some 15 projects are under preparation by members of LEUT. For further details of LASSO, see Ref. 18.

7. REFERENCES

1. Flury, W. 1973, Station-keeping of a geostationary satellite, ELDO/ESRO Sci. & Tech. Rev. 5, 131-156

2. Anselmi, A. 1981, A model for the radiation pressure effects on the SIRIO-2 satellite, ESOC/MAO WP No. 148

3. Woolard E.W. 1953, A redevelopment of the theory of nutation, Astron J. Vol. 58, No. 1

4. Flury, W. 1980, Laser ranging to SIRIO-2: A quasi-inertial reference frame for Earth satellite orbits, ESOC/MAO WP No. 135

5. Takeuchi, H. 1966, Theory of the Earth's interior, London, Blaisdell Publ. Co.

6. Escobal, P.R. 1975, Explicit analytic model for the Earth tide station coordinate deflections, JPL EM 391-624

7. Kaula, W.M. 1966, Theory of satellite geodesy, London, Blaisdell Publ. Co.

8. Wagner, C.A. et al 1977, Improvement in the geopotential derived from satellite and surface data (GEM 7 and 8), J. Geophys. Res., 82, No. 5, 901-914

9. Lerch, F.J. et al 1977, Gravity model improvement using GEOS-3 (GEM 9 and 10), GSFC, X-921-77-246.

10. Balmino, G. et al 1976, The GRIM 2 gravity field to the sixteenth degree and station coordinates from satellites and terrestrial data, J. Geophys. Res., 76, No. 20, 4855-4883

11. Gaposchkin, E.M. & Lambeck, K 1971, Earth's gravity field to the sixteenth degree and station coordinates from satellites and terrestrial data, J. Geophys. Res., 76, No. 20, 4855-4883

12. Gaposchkin, E.M. 1980, Global gravity field to degree and order 30 from GEOS 3 satellite altimetry and other data, J. Geophy. Res., Vol. 85, No. B12, 7221-7234

13. Merson, R.H. 1972, Geopotential coefficients for geostationary satellite orbits, RAE Tech. Rep. 72212

14. Allan, R.R. 1965, On the motion of nearly synchronous satellites. Proc. Roy. Soc. A, 288, 60-68

15. Munk, W.H. & Macdonald G.J.F. 1960/1975 The rotation of the Earth, Cambridge Univ. Press

16. Wilkins, G.A. (ed) 1980, Project MERIT. A review of the techniques to be used during Project MERIT to monitor the rotation of the Earth, Royal Greenwich Observatory.

17. Lambeck, K. 1972, Polar motion from the tracking of close earth satellites, Proc. of IAU Symposium No. 48 on Rotation of the Earth

18. Serene B. & Albertolini P. 1980, The LASSO experiment on the SIRIO-2 spacecraft, ESA J. 1980, Vol. 4